

## Josephson junctions with nearly superconducting metal silicide barriers

Yonuk Chong<sup>a)</sup>

Korea Research Institute of Standards and Science, Daejeon 305-600, Korea

N. Hadacek, P. D. Dresselhaus,<sup>b)</sup> C. J. Burroughs, B. Baek, and S. P. Benz

National Institute of Standards and Technology, Boulder, Colorado 80305

(Received 4 October 2005; accepted 26 October 2005; published online 23 November 2005)

We present a detailed study of the electrical properties of Nb-based planar Josephson junctions with superconducting metal silicide barriers, TiSi<sub>2</sub> and WSi<sub>2</sub>. While these nonhysteretic junctions are useful for voltage standard applications, they are also an excellent model system to study proximity coupling in junctions having a barrier with a finite superconducting transition temperature. These silicide-barrier junctions have excellent uniformity and controllability, but as opposed to junction barriers with no measurable superconducting transition, the critical current of these superconducting-barrier junctions is a strong function of the operating temperature near 4 K; we also discuss the impact of this temperature dependence on device applications. © 2005 American Institute of Physics. [DOI: 10.1063/1.2137992]

Nonhysteretic Josephson junctions have been used in various superconducting electronics applications. Although shunted tunnel junctions have been common with Nb-based superconductors, intrinsically shunted junctions became widely used with the advent of oxide-based high- $T_c$  superconductors.<sup>1</sup> It has been also found that they are particularly useful in Nb- and NbN-based voltage standard circuits. The superconductor-normal metal-superconductor junction,<sup>2,3</sup> in which a normal metal is sandwiched between two superconductors, is the most common intrinsically shunted junction system for these latter applications.<sup>4-6</sup> However, in some cases, the barrier material is also a superconductor with a transition temperature lower than either of the electrodes and lower than the operating temperature;<sup>7</sup> this is typically called an SS'S junction structure. In our search for improved Nb-based junctions for voltage standard applications we have found two such barrier materials with excellent characteristics, TiSi<sub>2</sub> and WSi<sub>2</sub>.

In this letter we present a Nb-based, metal-silicide-barrier junction as a model system to study the properties of the SS'S system. We show that it has good controllability in material and junction parameters, as well as electrical characteristics that are compatible with integrated device applications, particularly Josephson arrays. Compared to the MoSi<sub>2</sub> barrier, which is now used for highly integrated Josephson devices,<sup>8,9</sup> TiSi<sub>2</sub> and WSi<sub>2</sub> have higher conductivity at liquid helium temperature. Later we describe in detail the fabrication process and proximity theory analysis for the TiSi<sub>2</sub> barrier material.

The amorphous TiSi<sub>2</sub> film is dc sputter deposited at ambient substrate temperature from a sintered stoichiometric target. At low Ar sputtering pressures, films show compressive stress and the sheet resistivity has little dependence on deposition pressure with a minimum value around 210  $\mu\Omega$  cm. In this work, we focus mainly on the films deposited at 2 mTorr of Ar pressure, which gives the lowest room temperature resistivity. The resistivity is nearly constant from room temperature to 4 K (230  $\mu\Omega$  cm). However, the film undergoes a superconducting transition at  $T_{cN}$

= 1.72 K. Junctions are formed with the TiSi<sub>2</sub> between two *in situ* sputtered Nb layers, 300 and 160 nm thick, for bottom and top, respectively.

We assume that in our samples the barrier thickness  $d$  is much larger than the normal metal coherence length  $\xi_N(T)$  in the temperature range of interest. According to the conventional de Gennes theory, if a metal with a superconducting transition temperature  $T_{cN}$  is sandwiched between two superconductors with a critical temperature  $T_c > T_{cN}$ ,  $J_c$  depends on two variables, the normal metal thickness  $d$  and the temperature  $T$ , as<sup>1,10</sup>

$$\begin{aligned}
 J_c(d, T) &= \left[ \frac{\pi}{2e\rho_N\xi_N(T)} \frac{|\Delta_i(T)|^2}{k_B T_c} \right] \exp[-d/\xi_N(T)] \\
 &= J_{c0}(d) \left| \frac{\Delta_i(T)}{\Delta_i(0)} \right|^2 \frac{\xi_N(T_c)}{\xi_N(T)} \\
 &\quad \cdot \exp\left\{ -\frac{d}{\xi_N(T_c)} \left[ \frac{\xi_N(T_c)}{\xi_N(T)} \right] \right\}, \\
 d &\gg \xi_N(T), \quad T_{cN} < T < T_c,
 \end{aligned} \tag{1}$$

in which we used the expression for the normal metal coherence length in the dirty limit,<sup>1,11</sup>

$$\begin{aligned}
 \xi_N(T) &= \left( \frac{\hbar D_N}{2\pi k_B T} \right)^{1/2} \left[ 1 + \frac{2}{\ln(T/T_{cN})} \right]^{1/2} \\
 &\equiv \left[ \frac{\hbar D_N}{\pi k_B (T - T_{cN})} \right]^{1/2} \text{ if } (T - T_{cN})/T_{cN} \ll 1.
 \end{aligned} \tag{2}$$

Here  $\rho_N$  is the resistivity of the barrier,  $\Delta_i(T)$  is the order parameter at the interface, and  $D_N$  is the diffusion constant of the barrier.

Figure 1 shows the characteristic voltage  $V_c = I_c R_n$  (where  $I_c$  is the critical current and  $R_n$  is the normal-state resistance) at 4 K as a function of the TiSi<sub>2</sub> barrier thickness  $d$ . The TiSi<sub>2</sub> barrier thicknesses are nominal values calculated from the deposition time and the calibrated rate of 18.0 nm/min. We can fit the data to the curve  $V_c(d) = I_c R_n(d) = V_{c0}(d/\xi_N)e^{-d/\xi_N}$  with a prefactor of  $V_{c0} = 2.6$  mV and a normal metal coherence length of  $\xi_N(4 \text{ K}) = 7.1$  nm.

<sup>a)</sup>Electronic mail: yonuk@kriss.re.kr

<sup>b)</sup>Electronic mail: haus@boulder.nist.gov

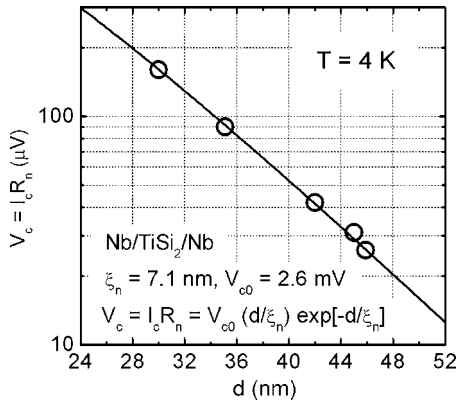


FIG. 1. Characteristic voltage  $V_c$  at 4 K as a function of the  $\text{TiSi}_2$  barrier thickness  $d$ . The thicknesses are inferred from the deposition time and the nominal deposition rate of 18.0 nm/min.

The critical current  $J_c$  can also be fit to  $J_c(d) = J_{c0} e^{-d/\xi_N}$  with a prefactor of  $J_{c0} = 235 \text{ mA}/\mu\text{m}^2$  and the same normal coherence length.

We assume that the S/N boundary of these  $\text{TiSi}_2$ -barrier junctions is in the rigid regime (no noticeable order parameter suppression in the superconducting electrodes) from our estimation of the suppression parameters  $\gamma$  and  $\gamma_B$ ;<sup>12</sup> we find  $\gamma = \rho_S \xi_S / \rho_N \xi_N = 0.04$  for the suppression in the superconductive region, and the order parameter discontinuity at the interface  $\gamma_B = R_B / \rho_N \xi_N < 0.6$ , where  $\rho_S(10 \text{ K}) = 4 \mu\Omega \text{ cm}$  and  $\xi_S(4 \text{ K}) = 17.5 \text{ nm}$  are the normal resistivity and the coherence length of Nb. The interface resistance  $R_B$  is measured to be less than  $10^{-10} \Omega \text{ cm}^2$ , which is extrapolated as a lower bound of the intercept of the plot of  $R_n A$  vs  $d$ , where  $A$  is the junction area.

Figure 2 shows the temperature dependence of the critical current density for different  $\text{TiSi}_2$  barrier thicknesses. The data fit well to Eq. (1) with  $\xi_N(T_c)$  and  $J_{c0}(d)$  as fitting parameters, and  $T_c$  is chosen to be 9 K for the best overall fit. We used the BCS energy gap for the temperature dependence of  $\Delta_i(T)$ , assuming a rigid interface. We can again confirm the rigid interface from the temperature dependence, since close to  $T_c$  the exponent  $\alpha$  of  $J_c \propto (T - T_c)^\alpha$  was estimated to be  $\sim 1.15$  for barriers of thickness 30 and 35 nm, for which

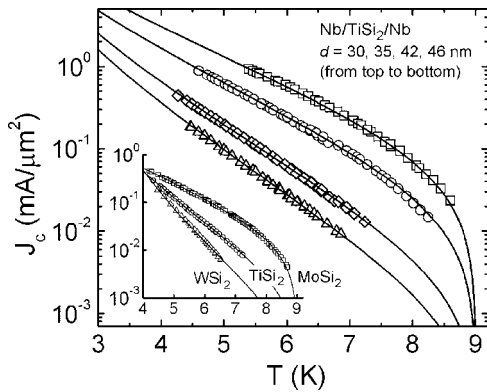


FIG. 2. Temperature dependence of  $J_c$  in junctions with different barrier thicknesses. Symbols are the measured data, and the lines are fit using Eqs. (1) and (2) with the fitting parameters given in Table I. The inset is a comparison of the steepness of the temperature dependence for junctions with three different barrier materials. These junctions have different barrier  $T_c$ 's but similar  $J_c$  values at 4 K, and the characteristic voltage  $V_c$ 's at 4 K are 48, 31, and 46  $\mu\text{V}$ , respectively, for  $\text{MoSi}_2$ ,  $\text{TiSi}_2$ , and  $\text{WSi}_2$  barriers. The  $\text{MoSi}_2$  barrier has been shown to have no superconducting transition down to 50 mK.

TABLE I. Values of the fitting parameters  $\xi_N(T_c)$  and  $J_{c0}(d)$  from the measured temperature dependence of the current density  $J_c$  for  $\text{TiSi}_2$  barrier junctions. Here  $V_c$ 's are inferred from measured  $I$ - $V$  curves, and  $\xi_N(4 \text{ K})$  is calculated using Eq. (2) and  $\xi_N(T_c)$ . The superconducting transition temperature  $T_c$  of the barrier was measured to be 1.72 K, and the  $T_c$  of the Nb yielding the best overall fit was 9.0 K.

$d$ (nm)	$V_c(4\text{K})$ ( $\mu\text{V}$ )	$\xi_N(T_c)$ (nm)	$J_{c0}(d)$ ( $\text{mA}/\mu\text{m}^2$ )	$\xi_N(4 \text{ K})$ (nm)
30	160	3.60	670	6.67
35	90	3.73	580	6.90
42	43	3.63	1700	6.73
46	26	3.87	1030	7.17

data points within  $(T_c - T) < 0.1 T_c$  are available. The resulting values of the fitting parameters are given in Table I. The normal coherence length is in good agreement ( $\sim 4\%$ ) with the value obtained from the barrier  $\xi_N$  thickness dependence. The apparently large scatter in the prefactors comes from uncertainty in estimating junction size. We note that the finite transition temperature of  $\text{TiSi}_2$  close to 4 K causes steep temperature dependence near 4 K compared to the case with nonsuperconducting barriers.

Note that we also find a good fit with the approximate form of  $\xi_N(T)$  given by Eq. (3), and that both fits overlap almost completely over the temperature range of interest. Even near  $T_c$ , where the approximation is poorest, we still get a coherence length that is within 6% of that from fitting with Eq. (2). This shows that the use of the approximate form of Eq. (3) is sufficient for practical characterization over a wide temperature range. Given  $\xi_N(T_c) \sim 3.7 \text{ nm}$ , using Eq. (2) we estimate the diffusion constant of  $\text{TiSi}_2$  to be  $D_N \sim 4 \times 10^{-5} \text{ m}^2/\text{s}$ .

Figure 3 shows the  $I$ - $V$  curves of a series array of 2000 double-junction stacks (total of 4000 junctions) at 4 K with 15 GHz of microwave bias. This sample has  $V_c = 31 \mu\text{V}$  and  $d = 45 \text{ nm}$  [ $d/\xi_N(4 \text{ K}) \sim 6.3$ ]. The large, flat Shapiro step implies good uniformity of the junctions, and it shows that the  $\text{TiSi}_2$  barrier junctions are compatible with integrated Josephson devices. For more complex circuits with more junctions, we also demonstrated a programmable Josephson voltage standard chip using these  $V_c = 31 \mu\text{V}$  junctions. The 1 V chip contains 33 705 junctions,<sup>9</sup> and has uniform constant voltage steps over 1.5 mA current range at a 13 GHz operating frequency. This current range is more than adequate for voltage standards applications, although at this reduced fre-

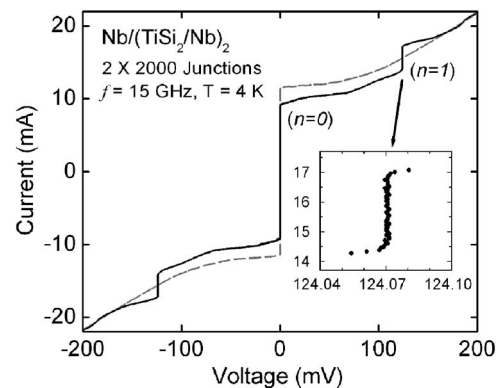


FIG. 3.  $I$ - $V$  characteristics of a series array of 2000 double-junction stacks with (solid) and without (dashed) 15 GHz microwave bias at 4 K. The array produces a flat Shapiro step with a current range of  $\sim 2.5 \text{ mA}$ . The inset shows that the Shapiro step is indeed flat and at the proper voltage.

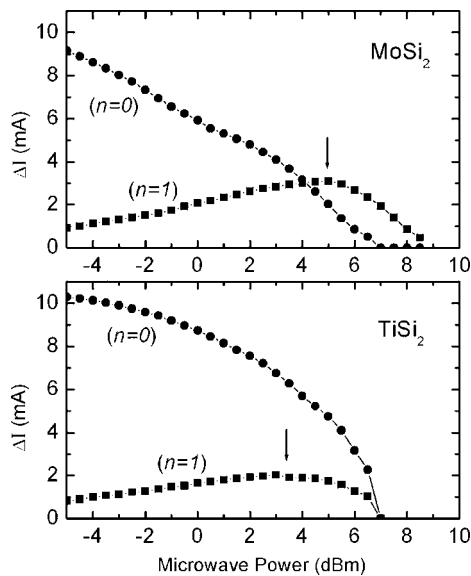


FIG. 4. Microwave response of the size of the critical current ( $n=0$ ) and first Shapiro step ( $n=1$ ) for (a) a  $\text{MoSi}_2$ -barrier junction array and (b) a  $\text{TiSi}_2$ -barrier junction array. Both arrays have 4400 junctions in series. The presented power dependences are measured at 13 GHz, but they show similar behavior for frequencies up to 18.5 GHz. The arrows indicate the power at which the current range of the first step is maximized.

quency the maximum output voltage is only 0.9 V.

Unfortunately, the operating margin is not as large as our conventional  $\text{MoSi}_2$ -barrier devices,<sup>9</sup> although from the  $I$ - $V$  curves the junction uniformity is comparable. We believe that the difference in behavior is due to significant heating that suppresses the critical current in the  $\text{TiSi}_2$  barrier junction, due to its finite  $T_c$ . For example, the microwave response of constant voltage steps in junctions with PdAu or  $\text{MoSi}_2$  barrier always shows that the first ( $n=1$ ) Shapiro step grows in size with increasing microwave power until the critical current is nearly suppressed, as shown in Fig. 4(a). In contrast, in  $\text{TiSi}_2$  junctions we observe that the microwave power required to maximize the first Shapiro step is lower than the power to minimize the critical current, as shown in Fig. 4(b). Furthermore, the microwave power at which all the constant voltage steps vanish is only slightly (10%) higher. These two effects are most likely due to a high total power dissipation and correspondingly elevated temperature for operation on the  $n=1$  step, and is a result of the steep temperature dependence of the critical current near the 4 K operating temperature, as shown in the inset of Fig. 2. We surmise that this effect, which would be a universal effect for SS'S junctions at high current bias, makes finite- $T_c$  superconducting barriers poor candidates for high density Josephson devices, where large heat dissipation is expected.

We also investigated another superconducting metal silicide barrier,  $\text{WSi}_2$ , which has a 2.85 K superconducting transition temperature and a  $230 \mu\Omega \text{ cm}$  room temperature resistivity. We fabricated junctions with barriers 38 and 49 nm thick, which respectively produced  $V_c=130$  and  $46 \mu\text{V}$ . Using the same analysis procedure as for the  $\text{TiSi}_2$  barrier on the measured electrical parameters as a function of temperature, we obtain for  $\text{WSi}_2$  a coherence length of  $\xi_N(4\text{K})=8.6 \text{ nm}$ . Because the  $\text{WSi}_2$  barrier has a higher  $T_{cN}$  than  $\text{TiSi}_2$ , the temperature dependence of the critical current is even steeper at 4 K than that of  $\text{TiSi}_2$ , as shown in the inset

of Fig. 2, hence, dramatically diminishing its usefulness as a barrier material.

We note that the SS'S junction structure is of special interest for high- $T_c$  superconductor junctions, in which the barriers are often also superconducting at some reduced temperature.<sup>1</sup> One of the widely used types of materials for high- $T_c$  superconductor junctions is a variation of the superconductor itself,<sup>13-16</sup> where the barrier materials have a reduced, but finite, superconducting transition temperature  $T_{cN}$  typically around 50 K and the junctions are operated above  $T_{cN}$ , usually at 77 K. If we compare  $\text{TiSi}_2$ - and  $\text{WSi}_2$ -barrier junctions with  $\text{MoSi}_2$ -barrier junctions,<sup>8</sup> we find that,  $\text{MoSi}_2$ , the barrier material with  $T_{cN}$  far below the operating temperature, gives superior performance for large-scale high-density circuits.

In conclusion, we have presented a quantitative analysis of the electrical properties of  $\text{TiSi}_2$ - and  $\text{WSi}_2$ -barrier SS'S Josephson junctions. These barrier materials form very uniform junctions, and typical fabrication procedures produce junctions with well-controlled electrical characteristics. Our measurements and detailed results on Nb-(Ti or W) $\text{Si}_2$ -Nb junctions show that their excellent uniformity makes them apparently useful barriers for large-scale integrated Josephson circuit applications. However, the strong temperature dependence of their electrical properties significantly reduces their performance compared to nonsuperconducting barrier junctions. This may be especially important for devices that are not operated in liquid cryogenics, where the operating temperature may fluctuate. In addition, we suggest that these two SS'S junction systems are excellent models in which to study the proximity effect for barriers with finite  $T_{cN}$ . We are optimistic that our analysis based on the de Gennes model is adequate to describe the behavior of these Nb-based junctions, and the model can be used to search for other useful barrier materials.

The authors thank Alan Kleinsasser for valuable discussions. This work was supported in part by the Office of Naval Research Contract Nos. N0001404IP20044 and N0001405IP20017.

<sup>1</sup>K. A. Delin and A. W. Kleinsasser, *Supercond. Sci. Technol.* **9**, 227 (1996).

<sup>2</sup>P. G. de Gennes, *Superconductivity of Metals and Alloys* (W.A. Benjamin, New York, 1966).

<sup>3</sup>J. Clarke, *Proc. R. Soc. London, Ser. A* **308** 447 (1969).

<sup>4</sup>S. P. Benz, *Appl. Phys. Lett.* **67**, 2714 (1995).

<sup>5</sup>M. Ishizaki, H. Yamamori, A. Shoji, P. D. Dresselhaus, and S. P. Benz, *IEEE Trans. Instrum. Meas.* **54**, 620 (2005).

<sup>6</sup>A. M. Klushin, R. Behr, K. Numssen, M. Siegel, and J. Niemeyer, *Appl. Phys. Lett.* **80**, 1972 (2002).

<sup>7</sup>J. Clarke, S. M. Freake, M. L. Rappaport, and T. L. Thorp, *Solid State Commun.* **11**, 689 (1972).

<sup>8</sup>Y. Chong, P. D. Dresselhaus, and S. P. Benz, *Appl. Phys. Lett.* **86**, 232505 (2005).

<sup>9</sup>Y. Chong, C. J. Burroughs, P. D. Dresselhaus, N. Hadacek, H. Yamamori, and S. P. Benz, *IEEE Trans. Instrum. Meas.* **54**, 616 (2005); *IEEE Trans. Appl. Supercond.* **15**, 461 (2005).

<sup>10</sup>P. G. de Gennes, *Rev. Mod. Phys.* **36**, 225 (1964).

<sup>11</sup>V. G. Kogan, *Phys. Rev. B* **26**, 88 (1982).

<sup>12</sup>M. Yu. Kupriyanov and V. F. Lukichev, *Sov. Phys. JETP* **67**, 1163 (1988).

<sup>13</sup>L. Antognazza, S. J. Berkowitz, T. H. Geballe, and K. Char, *Phys. Rev. B* **51**, 8560 (1995).

<sup>14</sup>L. Antognazza, B. H. Moeckly, T. H. Geballe, and K. Char, *Phys. Rev. B* **52**, 4559 (1995).

<sup>15</sup>B. Oh, Y. H. Choi, S. H. Moon, H. T. Kim, and B. C. Min, *Appl. Phys. Lett.* **69**, 2288 (1996).

<sup>16</sup>J. P. Zhou, J. T. McDevitt, and Q. X. Jia, *Appl. Phys. Lett.* **72**, 848 (1998).